Carbon Dioxide Concentrations and Efflux from Permanent, Semi-Permanent, and Temporary Subalpine Ponds

Amanda Gay DelVecchia [1,2,3] • Jared A. Balik [1,2] • Susan K. Campbell [1,3] • Brad W. Taylor [1,2] • Derek C. West [1,2] • Scott A. Wissinger [1,3]

Abstract

Small ponds account for a disproportionately high percentage of carbon dioxide emissions relative to their small surface area. It is therefore crucial to understand carbon flow in these ponds to refine the current global carbon budget, especially because climate change is affecting pond hydrology. High elevation ponds in the Elk Mountains of western Colorado are drying more frequently as the timing of snowmelt advances. We compared CO_2 concentrations and fluxes among ponds of different hydroperiods over diel sampling periods during the course of the 2017 open-water period. CO_2 concentrations were significantly negatively correlated with pond depth and averaged 77.6 ± 24.5 μmol L^{-1} (mean $\pm$ S.E.) across all ponds and sampling events. Ponds were up to twenty times supersaturated in CO_2 with respect to the atmosphere. Flux was highly variable within individual ponds but correlated with time of sampling and was highest at night. Flux averaged 19.7 ± 18.8 mg CO_2 m^{-2} h^{-1} across all ponds and sampling events. We also compared flux values obtained using modeled and empirical methods and found that widely-applied models of gas exchange rates using wind-based gas exchange (K) values yielded estimates of CO_2 flux that were significantly higher than those obtained using the floating chamber approach, but estimates of CO_2 flux using globally averaged convection-based K values were lower than those obtained using the floating chambers. Lastly, we integrated soil vs. water efflux measurements with long-term patterns in hydrology to predict how total season-long efflux might change under the more rapid drying regimes and longer seasons that are already occurring in these systems. Because soil CO_2 efflux averaged 277.0 ± 49.0 mg CO_2 m^{-2} h^{-1}, temporary ponds emitted 674.1 ± 99.4 kg CO_2 m^{-2} over the course of the 2017 season from ice-out to refreezing, which was over twice as much as permanent and semi-permanent ponds. Our results emphasize that contributions of CO_2 from small ponds to the global carbon budget estimates will vary with pond hydroperiod and sampling methodology, which have been overlooked given that most previous estimates were collected from limited sampling periods and from pond waters alone. Furthermore, pond CO_2 contributions are predicted to increase over time as pond areas transition from efflux from water to efflux from soil.

Keywords Carbon dioxide · Temporary ponds · Greenhouse gas efflux · Pond hydroperiod

✉ Amanda Gay DelVecchia
amanda.delvecchia@gmail.com

Jared A. Balik
jabalik2@ncsu.edu

Susan K. Campbell
campbells@allegheny.edu

Brad W. Taylor
bwtaylo3@ncsu.edu

Derek C. West
derekw28@gmail.com

Scott A. Wissinger
swissing@allegheny.edu

1   Rocky Mountain Biological Laboratory, PO Box 519, Crested Butte, CO 81224, USA

2   Department of Applied Ecology, North Carolina State University, Raleigh, NC 27695, USA

3   Department of Biology, Allegheny College, Meadville, PA 16335, USA

Introduction

Although inland waters comprise a small fraction of global surface area, the collective surface area of shallow freshwater lentic habitats (lakes, ponds, wetlands) emit approximately half of the annual carbon dioxide uptake of the oceans (Duarte and Prairie 2005). Of these freshwater systems, small ponds (<0.001 km^2) in the terrestrial landscape comprise 8.6% of global lentic surface area, but account for 15.1% of total CO_2 emissions from lentic systems (Holgerson and Raymond 2016), and slightly larger systems (0.002 to 0.01 km^2) comprise an additional 77% of global lentic surface area (Downing et al. 2006; Verpoorter et al. 2014). Small ponds, wetlands, and other shallow lentic habitats are potential carbon cycling hotpots because they have high inputs of terrestrial and aquatic vascular plant carbon, high rates of organic carbon burial in sediments, and high surface area to volume ratios (Downing et al. 2006; Cole et al. 2007). While inundated, these ponds provide a net efflux of CO_2 and store substantial organic carbon in anoxic sediments (Bridgham 2014) and when dry and oxygenated, the soils can release more carbon than the waters had released. However, temporary ponds are not explicitly considered in estimates of global small pond surface area (Downing et al. 2006) and estimates of CO_2 efflux from these water bodies generally consider efflux from the water itself. However, climate change has already and is predicted to continue shifting temperate alpine wetlands towards increasingly dry (more temporary) conditions that have the potential to release stored carbon, resulting in a positive feedback with climate change (Burkett and Kusler 2000; Lee et al. 2015). It is therefore important to understand how drying regime will affect carbon flux from these ubiquitous lentic systems (Obrador et al. 2018).

Estimates of CO_2 flux from pond systems are largely limited to studies of ponds that do not dry annually, and are most often measured indirectly using CO_2 concentrations (Holgerson and Raymond 2016; Bortolotti et al. 2016) rather than direct measurements (Laurion et al. 2010; Catalán et al. 2014; Kragh et al. 2017; Obrador et al. 2018). These estimates are also most commonly collected during short sampling periods during the day and over the course of the pond wetted period, despite evidence for diel (Hamilton et al. 1994; Cole and Caraco 1998) and seasonal variation in carbon flux (Cole and Caraco 1998). Total flux from a pond is most relevant when considering the entire pond area, or that which is wetted at the time of maximum fill or ice-out, as it transitions to minimum water levels over the course of a season or year. Measuring total flux from pond areas could involve changes in CO_2 flux from pond waters themselves, or a shift to flux from exposed pond sediments as parts or all of the pond sediments become exposed and/or aerated (Catalán et al. 2014; Obrador et al. 2018).

Hydroperiod, or the duration of surface water inundation of ponds and wetlands, provides a broad classification for studying how CO_2 flux from waters and from total pond area differs between ponds of different drying regimes (Jackson et al. 2014). In order to provide a general classification system, permanent ponds remain wetted throughout every season, semi-permanent ponds completely dry in some, but not other years, and temporary ponds dry annually. Pond hydroperiod is a major influence on pond ecology and ecosystem function (Power et al. 1988; Resh et al. 1988; Brooks 2009; Batzer and Sharitz 2014), and can be a stronger driver of pond nutrient and chlorophyll concentrations than biotic, spatial, or temporal factors (Magnusson and Williams 2006). Litter quality and hydroperiod interact to affect decomposition rates partially because invertebrate shredders prefer high quality, more consistently inundated litter (Baker et al. 2001; Battle and Golladay 2007; Inkley et al. 2008), but invertebrate and amphibian communities also differ along hydroperiod gradients because of varying abilities to cope with drying and/or the predators in permanent habitats (Batzer and Wissinger 1996; Wellborn et al. 1996; Strachan et al. 2014). Temporary ponds also tend to have higher surface area to volume ratios that allow more interaction between the benthic environment and the water column, leading to more rapid carbon cycling (Kelly et al. 2001; Kortelainen et al. 2006). Lastly, temporary ponds have a higher proportion of surface area that is aerated annually, and the few studies that have examined temporary pond flux have shown higher rates of CO_2 flux from exposed sediments (Catalán et al. 2014; Obrador et al. 2018).

Shallow lakes and ponds are especially sensitive to changes in snowmelt, precipitation, and evaporation (Corcoran et al. 2009; Tuytens et al. 2014) and pond hydroperiod is likely to be shortened by global climate change because of several mechanisms which decrease water supply and increase evaporative losses. Warmer winters decrease the amount of snowpack and alter precipitation patterns, making water inputs lower and less consistent (Barnett et al. 2005). Warmer temperatures and a shorter duration of snow cover allow for greater evaporation, increasing water loss from ponds (Carpenter et al. 1992; Arnell 1999). As a result, ponds whose hydrological budgets are dominated by snowmelt are becoming more temporary, drying earlier in the season and at a higher interannual frequency (Smol and Douglas 2007). As these transitions are occurring, despite clear differences in ecology between ponds of differing hydroperiods, we have an incomplete understanding of CO_2 dynamics that is characterized by a) limited data on natural diel and temporal variation in CO_2 flux for a given pond classification, especially given that flux is generally estimated from CO_2 concentrations rather than directly measured; b) a paucity of estimates of total flux over the wetted season that consider the proportion of a pond area that transitions to sediment flux rather than water flux; and c) a lack of baseline data on ponds that serve as sentinels of climate change, such as high-elevation ponds. In permanent ponds, CO_2 flux should be relatively low because much of the plant and animal material upon which microbial processing

depends falls below the aerobic-anaerobic boundary layer, resulting in a shift towards relatively slow anaerobic microbial processes associated with the early stages of peat formation (Clymo et al. 1998; Boon 2006; Bonaiuti et al. 2017). Temporary ponds are aerated annually, and thus soil organic carbon could be respired during the dry period.

The Mexican Cut Natural Preserve (MCNP) in the Elk Mountains of Colorado is a pristine subalpine study site, well-suited to address these uncertainties because it contains over fifty ponds of varying hydrology located in a high-elevation (3640 m) mountainside basin. Ecosystems at high elevations have high soil carbon content and therefore play an important role in the global carbon budget (Post et al. 1982). They are also considered sentinel systems for climate change at higher latitudes (Williamson et al. 2009; Wissinger et al. 2016). High-elevation ponds are missing from assessments of small pond CO_2 concentration and flux (Holgerson and Raymond 2016) but these ponds receive the majority of their annual precipitation as winter and spring snow, and thus are particularly vulnerable to shifts in the amount of snowpack and timing of melt (Serreze et al. 1999). Snowmelt timing in this region shifted a median of 2–3 weeks earlier between 1978 and 2007, with snow water equivalent declining by 3.6 to 4.1 cm decade^{-1} (Clow 2010). In 2012, snow depth was 50+ cm lower, snowmelt 28 days earlier, and early summer precipitation 12 cm less than the previous 10-year average across the region, reinforcing long-term trends we observe in those climate variables (Skordahl 2013). In this and other recent years with early snow melt, entire cohorts of species characterized as temporary-habitat specialists have perished in the face of extraordinarily early pond drying at our study sites (Lund et al. 2016).

With these changes in hydrologic patterns, we expect snowmelt-driven ponds to become increasingly temporary with continuing climate change. Thus, using the many ponds with different hydroperiods in close proximity at the Mexican Cut site (see Wissinger et al. 1999), our primary objective was to understand how CO_2 concentrations, flux rates, and total flux, as well as diel and temporal variation in concentration and flux values, compared across pond hydroperiods over the course of the open-water season. Secondly, we evaluated if widely-applied methods for studying flux encompassed this variation. We measured carbon dioxide concentrations and flux rates in twelve of the Mexican Cut ponds, four each of permanent, semi-permanent, and temporary classifications over the course of pond ice-out to the annual minimum (before ponds began to continuously refill and dry from late-season precipitation).

Study Site and Sampling Locations

All ponds were located within the Mexican Cut Nature Preserve in the Elk Mountains of central Colorado, a pristine, subalpine wilderness area owned by The Nature Conservancy and managed by the Rocky Mountain Biological Laboratory (Fig. 1) (Dodson 1982). We studied four ponds of each of three hydroperiod classifications: permanent, semi-permanent, and temporary (Wissinger et al. 1999). The ponds ranged in maximum wetted area (during the 2017 sampling period) from 900 to 7800 m^2. All were located within a radius of 0.2 km. Ponds thawed and became accessible at the end of June 2017 (Fig. 1a:1D).

We began diel aqueous CO_2 and flux sampling on July 18. At each pond, we identified a sampling location at the southern end that was accessible (within 1.5 m) from the shoreline and kept this sampling location consistent for all sampling events. We sampled ponds at a 1–2 week interval until August 30, 2017. On each sampling date, we conducted four rounds of sampling starting at 9 am, 12 pm, 9 pm, and 3 am the following day. We collected one sample from each pond for each sampling event. We also collected samples from different locations in the same ponds on a subset of sampling events in July to measure variation in aqueous concentrations and flux rates within ponds.

Sampling required approximately 3–4 h during each round, so exact times were not matched between ponds but each pond had four times of measurement over the course of a 24-h period. We were unable to collect measurements during precipitation events (which became frequent after August 30), which prevented operation of our sampling equipment and caused disturbance in the flux chambers.

We estimated pond depth to understand relative differences in volume and surface area:volume ratios between ponds. Pond depths were measured on August 9, 2017, and one average pond depth was calculated for each pond. For all permanent ponds and pond 8, depths were measured across five parallel, equally spaced width transects. For all other ponds, depths were measured across a perpendicular length and a width transect. Depths were recorded every four meters across pond 1, every 2 m across ponds 5, 8 and 12, and every meter for all other ponds. We measured the maximum wetted pond areas using Trimble GeoXT GPS units (< 50 cm accuracy) by walking the perimeter of each pond in the first two weeks of July before ponds started drying, and then calculating areas in ESRI ArcMap 10 (Table 1).

Methods

Aqueous CO_2 Concentrations: Sample Collection and Calculations

We collected samples for measurement of aqueous CO_2 concentrations by gently submerging a 500 mL glass culture bottle (Hybex media storage bottle) approximately 5–10 cm below the water surface and filling to approximately 5/6 volume. We capped bottles with black butyl rubber septa (McMaster
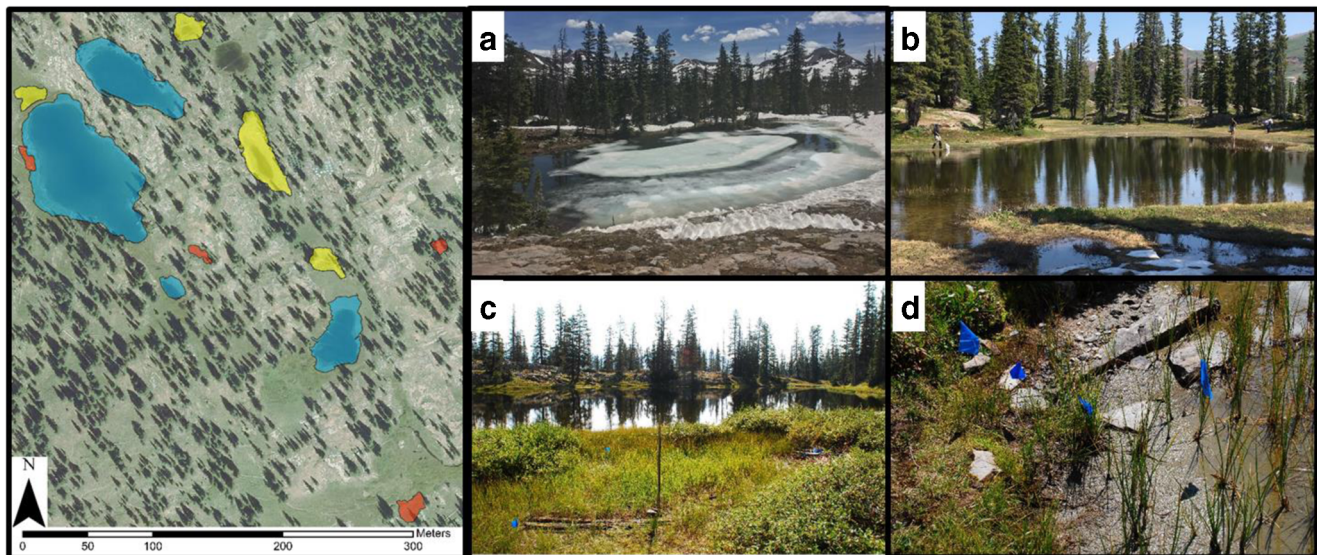
Fig. 1 (Imagery) Pond outlines recorded in July 2017 using Trimble GeoXT GPS unit overlaid on 2013 1-ft resolution imagery collected by Gunnison County. The southwest corner of shown location is located at 39°01′ 39″ N, 107°03′53″ W. Blue indicates permanent ponds, yellow semi-permanent, and red temporary. Pictures: A. On June 17, 2017, Mexican Cut pond MC12 (permanent) was mostly covered by ice. B. MC10 (semi-permanent) in late July 2017. MC10 did not dry in 2017. C. MC 42 and MC 1 in early September 2017. MC 42 was completely dried and the approximate center of the pond is indicated by the fencepost. MC 1 is permanent. D. An example of a transect to indicate drying dates in MC 42. Soil CO_2 efflux measurements were taken at multiple points in this location and other similar locations

Carr butyl rubber strips), inverted, and shook for two minutes in the field to allow for equilibration. We then measured headspace CO_2 concentration by removing 10 mL from the headspace with a 20 mL syringe and immediately injecting into a PP Systems EGM-5 Portable CO2 Gas Analyzer (PP Systems, Amesbury, Massachusetts, hereafter referred to as IRGA).

The IRGA unit was factory-calibrated to a maximum of 30 ppm error range which we verified using a 1000 ppm Scott gas analytical standard. However, sample injections yielded a systematic underestimate of CO_2 concentrations relative to direct measurement on the machine. Thus, we corrected all measurements of headspace CO_2 concentration using a linear relationship between injected and directly measured samples and standards ($R^2 = 0.9748$, Supplementary materials Fig. 1).

In order to understand the equilibration between an air headspace and dissolved CO_2 concentrations, we measured air CO_2 concentrations directly through the inflow on the IRGA. We averaged air CO_2 concentrations across all ponds for each time period (range: 413.1 ± 2.3 to 453.0 ± 2.4 ppm). To convert concentrations to partial pressures using the ideal gas law, we used an air temperature and pressure logger (Barologger Edge logger, Solinst Canada Inc., Georgetown, Ontario, Canada) to record air temperature and barometric

Table 1 Pond classifications and attributes. Values indicate averages over all sampling dates during daytime sampling sessions

Pond	Pond classification	Area (m^2)	Temp (°C)	Pressure (atm)	DO (mg/L)	DO (% saturation)	SPC	pH	Depth (m)
MC01	Permanent	5199.08	17.17	0.67	5.76	59.83	34.97	7.49	1.562
MC03	Permanent	183.36	14.86	0.67	5.21	51.84	38.20	8.38	0.45
MC05	Permanent	1194.95	14.93	0.67	6.37	63.15	35.40	8.41	0.676
MC06	Semi-permanent	287.79	14.57	0.67	5.69	55.98	13.52	7.71	0.68
MC08	Semi-permanent	993.52	16.40	0.67	5.29	54.14	8.97	7.82	0.701
MC10	Semi-permanent	314.21	14.17	0.67	5.25	51.00	10.98	8.15	0.61
MC12	Permanent	2013.20	15.19	0.67	5.23	54.30	6.44	7.53	1.467
MC13	Temporary	90.51	16.47	0.67	5.63	58.03	6.89	7.82	0.293
MC15	Temporary	81.15	12.47	0.68	5.41	50.91	10.84	7.73	0.444
MC22	Temporary	231.31	14.90	0.68	7.23	71.10	37.34	9.08	0.0275
MC42	Temporary	118.25	16.00	0.67	7.44	76.48	66.00	7.86	0.06
MC44	Semi-permanent	224.68	15.04	0.67	4.73	47.54	32.00	7.82	0.251

pressure every 10 min. We calculated the volume occupied by 1 mol of gas at each time of sampling as V_{Mt} as follows:

$$V_{Mt} = \frac{1}{P} * R * T$$

where R is the universal gas constant, equivalent to 0.08206 L atm mol^{-1} K^{-1}, T is the temperature in Kelvin, and P is the atmospheric pressure in atm. We used this value to convert ppm values to µmol/L concentrations of CO_2 in the headspace of each sample as C_{HS} as follows:

$$C_{HS} = \frac{ppm_{HS}}{V_{Mt}}$$

We used these measurements to calculate concentrations of CO_2 in the air headspace of each sampling bottle pre-equilibration using Henry's law. In order to calculate the Henry's law constant, K_H (mol L^{-1} atm^{-1}) for each sampling event, we recorded water temperatures every 10 min using a temperature and DO logger (MiniDOT logger, Precision Measurement Engineering Inc., Vista, California, USA) deployed at 10 cm depth in the deepest area of the pond, or as near to it as could be reached within 5.5 m of shore, then applied the equations given by Weiss (1974). We calculated initial aqueous CO_2 concentration in the sample as C_{aq} (µmol/L):

$$C_{aq} = \frac{\left\{ \left[(C_{HS} * V_{HS}) + \left(V_S * K_H * p_{HS} * 10^6 \right) \right] - (C_A * V_{HS}) \right\}}{V_S}$$

where V_{HS} is the volume of the headspace in the bottle (L), V_S is the volume of water sample (L), p_{HS} is the partial pressure of CO_2 in the headspace (atm), and C_A is the ambient air CO_2 concentration (µmol L^{-1}). We calculated the percent saturation of aqueous CO_2 relative to the atmosphere as follows:

$$\%Saturation\ CO_2 = \frac{C_{aq}}{p_A * K_H} * 100$$

where p_A is the partial pressure of CO_2 in the atmosphere calculated as the product of the measured ambient CO_2 concentrations and the barologger-measured air pressures.

During the day, we also measured dissolved oxygen concentrations, pH, and conductivity in the same locations from which we collected dissolved CO_2 samples using a handheld multiparameter water quality meter (YSI ProDSS submersible meter, YSI Incorporated, Yellow Spring, OH, USA).

Flux Rates: Sample Collection Using Floating Chambers and Calculations

We constructed floating chambers to measure CO_2 flux using a modified design from the methods of (Helton et al. 2014). Chambers were constructed from 10 L gas sampling bags

(Supelco analytical, Tedlar bags with push-pull valves) that were cut open at one end which was fit to a rectangular frame to obtain area measurements. The bag itself was anchored to a round polyethylene frame to keep each bag propped open. Chambers were thoroughly flushed with ambient air before setting on the ponds. At the time of sampling, the chamber was submerged approximately 1 cm in the water to create a seal, and chambers were tied approximately 1 m from pond shorelines to minimize turbulence from chambers being blown across the ponds. Our goal was to have time-specific measurements of flux that also minimized effects of turbulence that often occur suddenly at our study site. Diel variation in flux would not have been observable over long time periods of incubation, such as the 8 and 24 h incubations used by Helton et al. (2014), and long time periods would increase the probability of encountering sudden weather events that could bias results. We also did not want to leave chambers on ponds for short enough times that short term (< 1 h) temporal variability might affect how we interpreted differences between time periods, and additionally short incubation times would have required reducing the number of ponds we could sample, although accumulation rates have been shown to be linear in short incubations as well (Catalán et al. 2014; Obrador et al. 2018). Therefore, we left the chambers on the ponds for one to two hours during each sampling session, an intermediate and feasible incubation time for assuming a linear accumulation rate, similar to the 25–60 min incubation time used by Laurion et al. (2010). Given weather variability at Mexican Cut, extended incubations would have had a higher probability of disturbance or lost measurement points.

We sampled chambers by connecting the push-pull valve on each bag to vinyl tubing connected to the IRGA intake valve, then opened the push-pull valve and allowed the internal pump on the IRGA to flow at 270 to 280 cm^3 minute^{-1} until measurements stabilized (approximately 40–60 s). Measurements remained stable within 5 ppm over the time of sampling (1–2 min), and the gas sampling bags had some flexibility to keep a constant pressure over the time that 270–560 ml of gas were being run through the chamber.

We calculated the total moles of gas in each chamber for each sampling time using the ideal gas law and the temperature and pressure measurements that had been logged every ten minutes by the barologgers. We were thus able to standardize ppm values recorded using the IRGA to the change in the amount of CO_2 present in the chamber (µmol) as Δ_{co_2} as follows:

$$\Delta_{co_2} = \left(ppm_f - ppm_i \right) * N_{total}$$

where ppm_f is the final ppm measurement from the chamber, ppm_i is the initial ppm measurement from the chamber, and N_{total} is the total number of moles in the chamber at a given

measurement time. We calculated the rate of CO_2 flux (μmol m^{-2} min^{-1}) as follows:

$$Efflux_{CO_2} = \frac{\Delta_{co_2}}{A_C * t_{inc}}$$

where Δ_{co_2} is the change in the amount of CO_2 present in the chamber (μmol), A_C is the chamber base area (m^2), and t_{inc} is the incubation time (minutes).

Flux Rates: Estimating Flux Rates Using Published Models

In order to relate floating chamber measurements of CO_2 flux to estimates of CO_2 flux collected using either wind-based models or convection-based models, both commonly applied methods in pond studies, we estimated diffusive flux of CO_2 using the following equation:

$$Flux = K_{CO_2}(C_{aq} - C_{eq})$$

where K_{CO2} is the gas-specific exchange coefficient, C_{eq} is the concentration of dissolved CO_2 if in equilibrium with the atmosphere, and C_{aq} is the measured CO_2 concentration near the water surface. K_{CO2} was calculated using an expression of the CO_2 specific Schmidt number (Sc) as follows:

$$K_{CO_2} = K_{600}\left(Sc/600\right)^{-b}$$

Where b = 0.66 for wind speeds <3 m/s or b = 0.5 for wind speeds >3 m/s. The Schmidt number was found using the equation given by Wanninkhof 1992:

$$Sc(CO_2) = 1911.1 - 118.11T + 3.4527T^2 - 0.04132T^3$$

Where T is temperature (°C). K_{600} was the gas exchange coefficient (cm h^{-1}) normalized for CO_2 at 20 °C in freshwater with a Schmidt number of 600, estimated using two methods based on wind or convection models. Using the wind-based model, we applied the equation of Cole and Caraco (1998):

$$K_{600} = 2.07 + \left(0.215 \times U_{10}^{1.7}\right)$$

Where U_{10} is the wind speed at 10 m height. We used wind speeds collected by the RMBL weather station at Mexican Cut, located at a maximum distance of 270 m from the farthest sampling location (Billick n.d.). To apply convection-based model estimates, we followed the methods of Holgerson et al. (2017), which used an average K_{600} from temporary ponds in Connecticut for ponds <0.001 km^2 (Holgerson et al. 2017) and an average K_{600} for small ponds reported in Read et al. (Read et al. 2012) for ponds >0.001 km^2 and < 0.01 km^2 (0.48).

We also calculated an empirical K value by calculating a factor relating chamber-measured flux values to the difference in equilibrium and measured aqueous concentrations for each estimation method. We used a basic linear regression with a forced intercept of 0 to fit the measured or calculated flux values to the differences in concentrations for each efflux estimation method (floating chambers, convection-based, wind-based). This made it possible to report a directly comparable average K for each method.

Soil CO_2 Flux

We measured pond soil CO_2 flux on August 17, September 1, and September 14 from 10 ponds across all classifications. Our sampling was somewhat opportunistic because we could only collect efflux samples from exposed soils, or those in which the water table was below the ground surface, and this made it difficult to sample some locations immediately after rain events. Each time we measured pond soil CO_2 flux, we also measured soil CO_2 flux from soils <1 m outside of the maximum wetted pond margin for baseline estimates of soil CO_2 flux at Mexican Cut ($n = 15$). We collected measurements along a transect from the furthest dried margin of the pond to the current pond water edge. We placed flags to indicate pond water edge at dates throughout the season, and thus were able to sample between flags to collect measurements representing different times since initial soil drying.

We used a soil respiration chamber (SRC-2, PP Systems) to measure soil respiration along these dried pond margins and throughout temporary ponds that dried completely between August 17 and September 14. The chamber included a fan to recirculate air within the chamber, while the IRGA internal pump withdrew samples for measurement of CO_2 concentrations from the chamber. Ambient CO_2 concentrations within the chamber itself were measured before measurement of flux to allow verification that the chamber was completely flushed before sampling. After a 1-min incubation period, a quadratic relationship was assessed for the change in chamber CO_2 concentration over time to allow for an initial stabilization period and to ensure that leakage was minimal (if any) as follows:

$$C = a + bt + ct^2$$

where C is the concentration (ppm) in the chamber at time t (seconds). Variables a, b, and c are empirically determined coefficients for each chamber incubation used as follows. The true flux rate was calculated from $\partial C/\partial t$ at time $t = 0$. Thus, using $\partial C/\partial t = b + 2ct$, at T = 0, $\partial C/\partial t$ = b. A comparison of b and ct yielded an estimate of leakage; ct must be <20% of b or the relationship was deemed nonlinear and the chamber incubation was redone.

Estimating Total Pond Flux over the 2017 Season

Pond CO_2 flux measurements are generally collected from permanent ponds so total CO_2 flux estimates that include transition

from aqueous to terrestrial over the period from ice-out to refreezing are rare. However, total flux from a pond includes both the pond water and the soil that becomes exposed over the course of the season, and as the wetted section of the hydroperiod shortens, flux transitions from water to sediment. Thus, we estimated flux from entire pond areas over the season to compare between ponds of varying hydroperiod. We defined the "season" as the total time from ice-out to pond refreezing.

Open water days have been estimated since 1990 at Mexican Cut based on melting dates in spring, drying dates in summer, and freezing dates in autumn (summarized in Wissinger et al. 1999). Since 2004, data loggers (TruTrack WT-HR; Intech Instruments, New Zealand) have continuously recorded water depths, temperatures, and air temperatures at a subset of the ponds, including those used in this study. We used the logger data to determine annual dates of each pond's ice-out, drying, re-inundation, re-freezing, and inundated growing season length (Wissinger & Balik unpub.). Briefly, ice-out dates were identified as the first dates when water temperature increased from a frozen temperature (≤ 0 °C) and remained above freezing for 24 h. Drying dates were identified when water depth declined to a value ≤ 0 cm and water temperature equaled air temperature, indicating that both thermistors were reading air temperature. The pond wetted duration length was calculated as the difference between the first drying date and the ice out date, but could have been underestimated for temporary ponds if they refilled substantially before the freeze date. For semi-permanent and permanent ponds that did not dry, re-freezing dates were detected when water temperatures declined to a frozen temperature (≤ 0 °C) for longer than 24 h. For these habitats, the entire growing season length was calculated as the difference between the freezing date and the ice out date. Annual datasets for each pond were manually checked twice to verify all ice-out, drying, and re-freezing dates used to calculate growing season lengths, or the total time over which we estimated efflux from the combination of pond water and progressively exposed soils in each pond area.

In order to assess changes in water vs. exposed soil area over the season, we placed flags to mark pond margins at the start of the season (while ponds were at their maximum water levels) and on each sampling date thereafter on transects from the pond margin toward the approximate center of the pond. We measured the distance between flags at the end of the season. Of the 36 total transects that were placed, 23 had >3 flagged locations. We tested the validity of a linear rate of drying by fitting linear regressions for each of these transects (total dried distance vs. date). Because the R^2 values for these fits averaged 0.83, we assumed an approximately linear rate of drying in order to estimate changes in pond area over the course of the season.

In ArcMap 10, we placed markers on the GPS-collected pond shapes to indicate the location of initial flags. We then used the "scale" function to test what percentage of area decrease in each pond would cause the observed difference in flag locations along the transect by the end of the season. The "scale" function allows a user to specify a center point for a polygon, which we specified as the deepest portions of the pond basins, then specify a percentage change in area. We tested percentages of pond area shrinkage, then compared the new polygon margins to transects distances to understand what percentage change in area corresponded to the observed drying distances along transects. We used this approach because the ponds are extremely irregularly shaped, and this allowed us to keep the integrity of the pond shape to calculate the best possible estimate of shrinking pond areas. We fitted a line between the initial area at the time of melting and the final pond area on September 14, 2017, or for the temporary ponds the time of drying, to fit a line which allowed us to calculate a slope which estimated the rate of drying. We integrated under these curves over the wetted, open water period, which yielded an estimate of total area-days of water. Because we did not have direct measurements of the total open water period for 2017, we used the average season length, minimum season length, and maximum season length from the past years of data logger depth information (Supplementary Table 1). In addition, to account for potential changes in total efflux that could result from refill events, we used the average number of days per year that any depth of water (>1 mm over ground surface for at least one day) had been recorded in the ponds after the initial drying date (in temporary ponds) and assumed that the ponds had been refilled completely for this number of days, taking the most conservative approach possible in estimating total efflux given our limitation in not being able to extrapolate areal pond coverage from depth estimates. Thus, we included full areal coverage by water for any refill days recorded (all included in Supplementary Table 1). There were no refilling events in semi-permanent or permanent ponds. We subtracted the total wetted area days from the total potential area days over the entire season based on the maximum pond area and time to freezing to estimate total area-days of soil. Because flux measurements were highly variable within ponds, we estimated CO_2 flux using the overall mean from each pond soils and waters, respectively, stratifying by date of collection and pond (stratified means and variance, Thompson 2012).

Statistical Analyses

All statistical analyses were performed in R 3.2.4 (R Core Team 2016). We treated time of day as a circular variable using the function sin(decimal time × pi). We log-transformed CO_2 concentrations, which were highly right-skewed, to improve normality. We calculated site-wide means and variance estimates by stratifying measurements by pond (Thompson 2012).

We evaluated linear mixed effects models built in R package "nlme" (Pinheiro et al. 2014) by comparing AIC scores and log-likelihood values (Akaike 1998). Each model included pond as a random effect. We tested for significance of time of day, date of sampling, pond hydrologic classification, and pond depth using analysis of variance (ANOVA). In tests for differences between pond hydroperiod types, we also tested for improvement to models using interaction terms between pond type and time of day terms. We calculated marginal and conditional r-squared values for models using package "MuMIn" (Barton and Barton 2018).

In order to present site-wide means and standard error calculations that were not biased by number of observations per pond or sampling period, we first stratified observations by ponds and sampling periods (the four time periods of sampling during which we collected samples) (stratified means and variance, Thompson 2012). Unequal sampling effort in these strata was occasionally caused by storms.

Results

Differences in CO_2 Concentration, Saturation, and Flux Rates among Ponds of Different Hydroperiod, Time of Day, and over the Ice-Free Season

Mean CO_2 concentration across all ponds, sampling dates, and time of day was 77.6 ± 24.5 (SE) μmol/L ($n = 219$). Standard error in aqueous CO_2 concentrations across individual ponds averaged 3.2 μmol L^{-1} with a coefficient of variation of 12.2%. Mean CO_2 saturation was $625.9 \pm 193.9\%$ SE (range 10 to 2217) and followed patterns in CO_2 concentrations. Concentrations did not significantly differ between pond classifications (ANOVA $F_{2,9} = 2.6532$, $p = 0.124$) (Table 2) but permanent pond CO_2 concentrations were lower than both semi-permanent and temporary ponds (post-hoc Tukey test, $p = 0.067, 0.092$ respectively, Fig. 2a). Differences between pond classifications were largest on the July 31st and August 14th sampling dates.

We analyzed pond CO_2 concentrations by including pond classifications, time of day, the maximum pond depths, and day of the year as independent variables in linear mixed effects models that included the pond as a random effect to account for unknown variation between individual ponds. We compared models using log-likelihood values and AIC scores. The proportion of variance explained by pond compared to total variance in the dataset was 0.46, thus justifying the inclusion of pond as a random effect. Random intercepts models were consistently better fits based on AIC than random slopes models.

Pond water depths differed by pond classification ($F_{2, 9} = 5.304$, $p < 0.030$). Pond depths made the most improvement to the null model which only included the random effect of pond (Table 3). Neither pond classification nor the interaction between pond classification and depth improved the null model. The best model included pond depth and a continuous autocorrelation function of the time of day and date of collection in each pond, and showed that pond CO_2 concentrations tended to decrease with depth. The inclusion of depth improved the AIC (predictive power), but did not improve the conditional R^2 because depths were unique to individual ponds already included in the random effects.

Using the floating chambers, standard error in CO_2 flux rates within ponds was highly variable, with a standard error of 14.7 mg CO_2 $m^{2\ h-1}$ and a coefficient of variation of 48.5%. The mean $\pm$ 1 SE CO_2 flux rate across all ponds and sampling events (i.e. time of day and date), stratified by pond and sampling time, was 19.7 ± 18.8 mg m^2 h^{-1}. Differences in flux rates among pond classifications were not significant ($F_{(2, 9)} = 0.8223$, $p = 0.470$). There were no consistent changes in CO_2 flux over the course of the season, but flux estimates were generally lowest during the 9 am sampling period and highest during the 3 am sampling period (Fig. 2b). The maximum change in CO_2 flux predicted over the course of the day was 46.0 mg CO_2 $m^{2\ h-1}$ (Supplementary Fig. 2).

We analyzed pond flux rates the same way we analyzed concentrations. Random intercepts models were also consistently better fits based on AIC than random slopes models so we reported only random intercepts models in Table 4. Correlation between flux observations that were collected from the same pond, over any sampling date, was 0.10. The best model included time of day as the only fixed effect and a continuous autocorrelation function of the time of day and date of collection in each pond. Time of day was a significant predictor of flux (Fig. 2b) in the best fit model ($F_{(1, 195)} = 22.54$, $p < 0.001$). An equivalent model included the date of collection.

Table 2 Mean and standard error of each measurement for each pond type

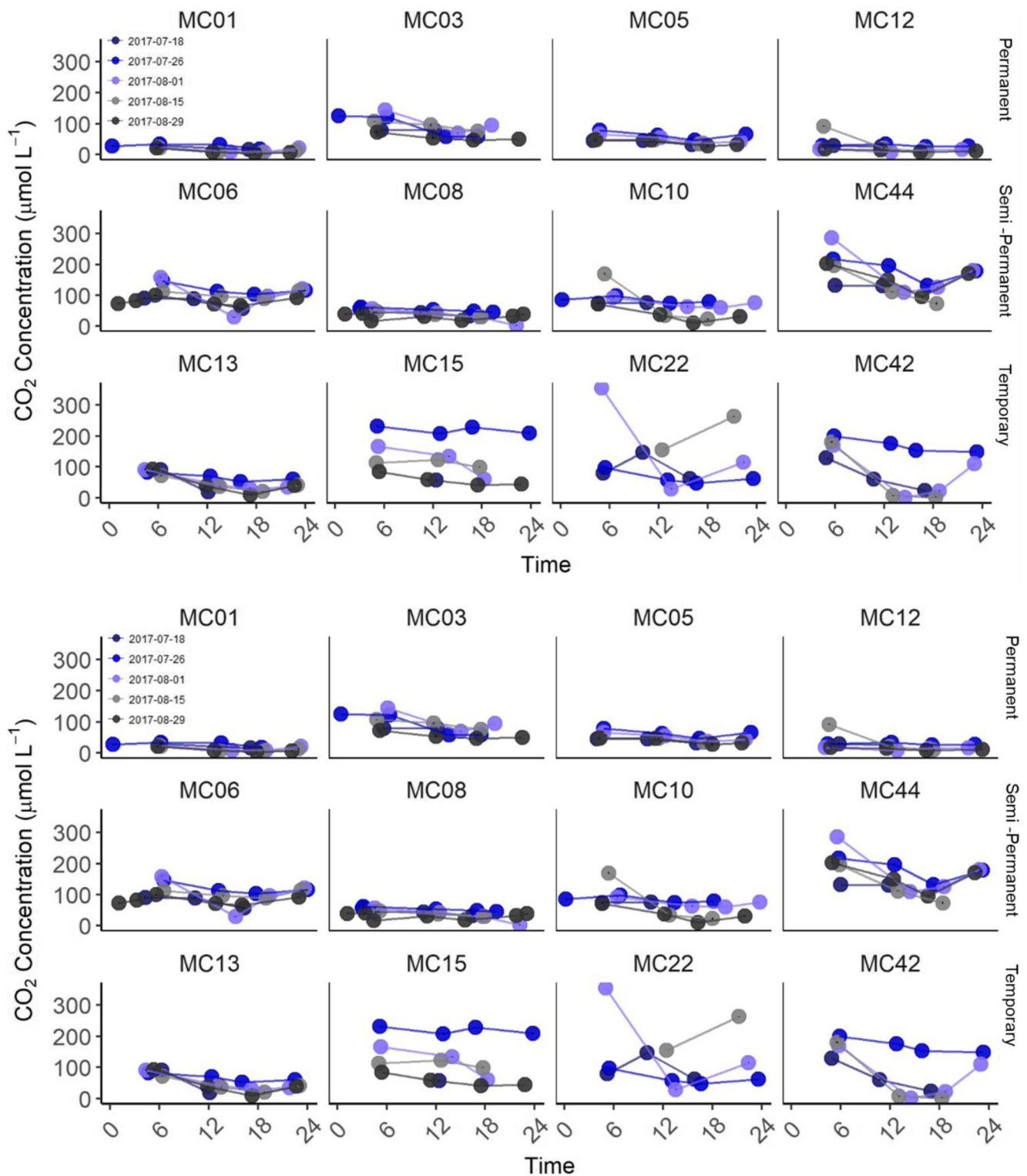|	Concentration (μmol CO_2/L)	Saturation (% CO_2)	CO_2 per unit area (mol CO_2 m^{-2})	Flux (mg $CO2/m^2hr$)
Permanent	47.1 ± 8.4	324.3 ± 67.7	35.6 ± 8.9	11.0 ± 18.6
Semi-permanent	84.7 ± 15.1	723.6 ± 121.3	45.7 ± 7.9	29.1 ± 18.9
Temporary	99.7 ± 47.6	797.1 ± 377.8	18.5 ± 5.7	19.2 ± 25.2

Fig. 2 Patterns in CO_2 concentrations and flux over the diel sampling period and with pond classification. "0" and "24" both indicate midnight

Measured Flux vs. Wind Speed and Temperature Based Models

Flux chambers were kept in a consistent location at all sampling times and were collected from directly above where aqueous CO_2 concentrations were measured. We compared directly measured flux rates (using the floating chamber technique) to flux rates modeled using wind-based and convection-based averages from other studies. We calculated an empirical K_{CO2} value by relating chamber-measured flux

Table 3 Mixed effects models of log-transformed CO_2 concentrations, including the best and initial model AIC scores and log-likelihood values as well as all models with two AIC units of the best fit model, listed in order of increasing complexity. Bold variables were significant in ANOVA tests (F test $p < 0.05$). ACF indicates the autocorrelation function of the date and time of sampling in each pond. All models included the pond as a random effect except the first (indicated). Variable values, standard errors, and t-test statistics are displayed for the underlined model, which was the best fit. Correlation between measurements from the same pond was 0.46

Model fixed effects			AIC	Log-likelihood	Marginal R^2	Conditional R^2
None (null model)			480.5	−237.3	NA	0.459
Depth			471.6	−231.8	0.286	0.454
Depth + ACF			437.4	−213.7	0.283	0.411
Depth + ACF + Time			437.9	−213.0	0.287	0.419
Variable	Value	Std Err	DF		t	p
Random intercepts: pond			193		23.953	<0.0001
Depth	−1.103	0.256	10		−4.309	0.0015

values to the difference in equilibrium and measured aqueous concentrations using a linear regression with a forced intercept of 0. Our empirically calculated K_{CO_2} value of 0.826 cm h^{-1} ($R^2 = 0.58$, F = 309.2, p < 0.001, $n = 229$) was lower than the wind-based model K_{CO_2} value of 1.698 cm h^{-1} but higher than the convection-based model K_{CO_2} value of 0.261 cm h^{-1} (Figs. 3). In both cases, the difference between measured and modeled flux estimates was highest at high levels of CO_2 saturation relative to atmospheric equilibrium, but the wind-based model and floating chamber approach were more similar at these high concentrations. Because differences between methods could have arisen from limitations in each of the methods or from an ecological explanation, we compared residuals between the floating chamber approach and each of the estimation methods to other variables. In order to test if wind speed might contribute to higher estimates from the wind based model relative to chambers, we used the wind speeds collected from the weather station at this location. In order to test if net ecosystem productivity might have contributed to higher uptake of CO_2 than the model explained, we used net ecosystem productivity estimates collected using the DO loggers (DC West and BW Taylor, unpublished data).

Wind speeds did not explain variation in the residuals for either model (wind: $R^2 = 0.0004$, $F_{(1, 227)} = 1.113$, $p = 0.292$; convection: $R^2 = 0.001$, $F_{(1,227)} = 0.293$, $p = 0.589$). Estimates of net ecosystem productivity obtained using hourly measurements of dissolved oxygen and temperature (DC West and BW Taylor, unpublished data) explained 9.2% of the variation in the residuals from the wind model ($F_{(1,227)} = 23.162$, p < 0.001) and 3.1% of the variation in the residuals from the convection model ($F_{(1,227)} = 7.195$, $p = 0.007$). Thus, neither wind speeds nor estimates of net productivity explained a substantial fraction of the differences in floating chamber vs modeled estimates.

CO_2 Flux from Pond Water and Previously Wetted Soils during the Ice-Free Season

We measured pond soil CO_2 flux on August 17, September 1, and September 14 from ten ponds across all classifications opportunistically as pond soils became exposed (water table below soil surface). Pond soils were exposed from 1 to 65 days, but the time exposed did not have a significant effect on soil CO_2 flux values ($F_{(1,108)} = 1.306$, $p = 0.255$). The

Table 4 Mixed effects models of CO2 efflux rates, including the best (underlined) and initial model AIC scores and log-likelihood values as well as all models with two AIC units of the best fit model, listed in order of increasing complexity. Bold variables were significant in ANOVA tests (F test p < 0.05). ACF indicates the autocorrelation function of the date and time of sampling in each pond. All models included the pond as a random effect except the first (indicated). Variable values, standard errors, and t-test statistics are displayed for the underlined model, which was the best fit. Correlation between measurements from the same pond was 0.11

Fixed Effects	AIC		Log-likelihood	Marginal R^2	Conditional R^2
None (null model)	2153.4		−1073.7	NA	0.114
Time	2134.2		−1063.1	0.086	0.200
Time + ACF	2129.2		−1059.6	0.087	0.198
Time + Date + ACF	2130.0		−1059.0	0.096	0.208
Variable	Value	Std Err	DF	t	p
Random intercepts: pond			195	32.157	<0.0001
Time	−45.963	9.680	195	−4.748	<0.0001

Fig. 3 Measured pond water CO_2 flux vs. CO_2 flux modeled using convection (Holgerson et al. 2017, white) or wind (Cole and Caraco 2007, grey). The solid black line indicates a 1:1 relationship
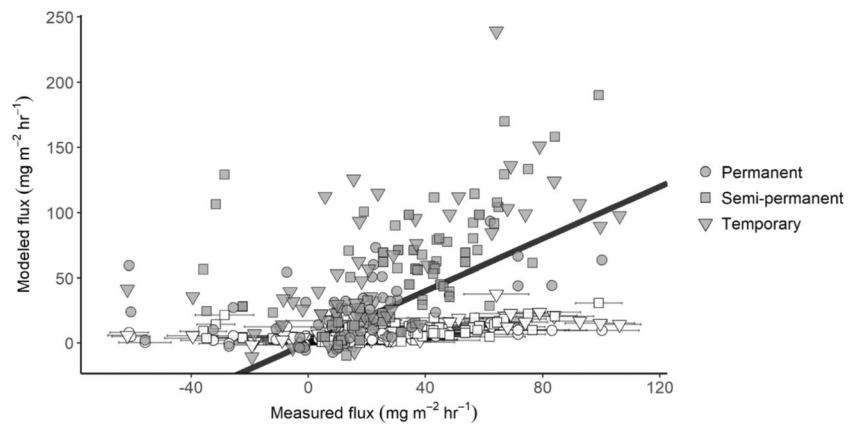
mean ± 1 SE soil CO_2 flux across all pond soils (stratified by pond) was 276.96 ± 48.99 mg m^{-2} h^{-1} ($n = 112$), equivalent to approximately 8.4 times the pond water flux rate. The mean ± 1 SE soil CO_2 flux from non-pond soils (baseline) was 668.21 ± 76.97 mg m^{-2} h^{-1} ($n = 14$), equivalent to approximately twenty times the pond flux rate.

Over the course of the entire season in 2017 from ice-out to re-freezing of permanent ponds assuming an average season length of 165, 147, and 136 days for permanent, semi-permanent, and temporary ponds respectively, CO_2 flux per unit area in temporary ponds was more than twice that of permanent and semi-permanent ponds in all scenarios (Fig. 4). The mean ± 1 SE seasonal flux from permanent ponds was 246.0 ± 47.21 kg m^{-2}, from semi-permanent ponds 178.4 ± 11.0 kg m^{-2}, and from temporary ponds 674.1 ± 99.4 kg m^{-2} (Table 5). Semi-permanent ponds had smaller areas than permanent ponds, but similar flux rates and length of open-water period, resulting in slightly lower total seasonal flux. Because of the higher CO_2 flux from soil than water, ponds with the shortest period of inundation yielded the highest season-long flux estimates.

Discussion

Differences in CO_2 Concentration, Saturation, and Flux Rates among Ponds of Different Hydroperiod, Time of Day, and over the Ice-Free Season

CO_2 concentrations in the Mexican Cut ponds were in the lower end of the range of values reported for similarly small temporary and permanent ponds, but the Mexican Cut is both a higher elevation and lower latitude than the majority of ponds previously studied (Holgerson and Raymond 2016) (Table 6). All ponds also had CO_2 flux rates significantly lower than those reported for ponds of similar size at lower elevations (Holgerson and Raymond 2016). These subalpine ponds also have low allochthonous carbon and nutrient input and thus might have lower rates of both productivity and respiration (Elser et al. 2009). Furthermore, these ponds likely have lower temperatures than lower elevation counterparts, also limiting respiration. The range of pond CO_2 saturation values, however, was similar to that of other ponds and small lakes, which are known to be supersaturated (Cole et al. 1994;

Fig. 4 CO_2 total efflux per square meter per pond over the 2017 season estimated using the average season length (ice-out to re-freezing) for each pond classification (Permanent: 165 days, Semi-permanent: 147 days, Temporary: 136 days). Arrows represent range of estimates using the minimum and maximum season length recorded over the last decade for each pond classification (Supplementary Table 1)
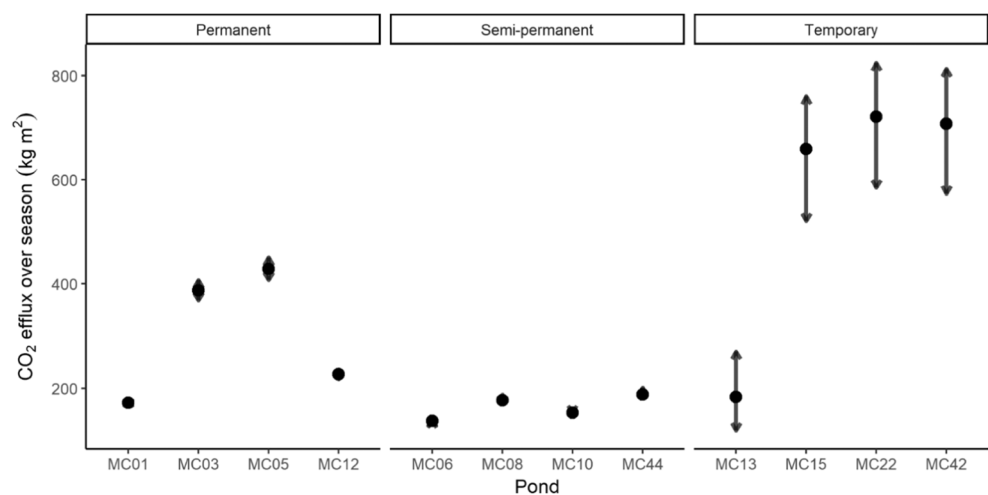
Table 5 Means and standard errors for estimates of total CO_2 efflux per square meter over the entire 2017 season for each pond classification

Season Length (days)	Permanent (kg m^{-2})	Semi-permanent (kg m^{-2})	Temporary (kg m^{-2})
Minimum	289.4 ± 58.3	160.3 ± 58.3	505.6 ± 82.1
Average	303.7 ± 61.9	178.4 ± 11.0	631.5 ± 95.5
Maximum	318.3 ± 65.8	197.3 ± 12.7	723.1 ± 103.4

Hamilton et al. 1994; Cole et al. 2000; Holgerson 2015). The discrepancy between relative concentrations and saturation values is consistent with the subalpine ponds having approximately ~67% of the atmospheric pressure found at lower elevation ponds.

When we compared ponds of differing hydroperiods, we found that temporary and semi-permanent ponds had the highest concentrations. Semi-permanent ponds had higher amounts of dissolved CO_2 per unit surface area in July (when depths were measured) than temporary ponds, despite having similar concentrations. If sediment respiration were driving CO_2 concentrations as described by Kortelainen et al. (2006), temporary ponds could have the highest amount of CO_2 per unit area because they are shallower. Our findings were not consistent with that prediction, so it is possible that water column respiration might also be contributing to CO_2 concentrations or that the temporary ponds might equilibrate more rapidly with the atmosphere because of their lower volumes. The possibility that water column respiration could be an important contributor to overall CO_2 concentrations was consistent with results from our linear mixed-effect model fits, which revealed that pond depth was highly correlated with pond type and was the best predictor of CO_2 concentrations.

Pond CO_2 concentrations did not vary significantly over the diel sampling period or over the course of the season, but flux rates did vary significantly with time of day. Other studies that have considered diel variation in CO_2 concentrations have found varying results: Cole and Caraco (1998) only found significant diel variation in the midsummer sampling period, whereas Hamilton et al. (1994) found differences from 10 to 80 μmol/L between dawn and dusk. Diel variation in CO_2 flux might be case-specific but merits further study because the vast majority of studies are conducted during the daytime over short sampling periods, which could lead to bias. However, because CO_2 concentrations, which should be directly related to flux, did not also have a diel pattern, we could not distinguish between some influence on the chambers themselves that changed over the sampling period (e.g. surface turbulence caused by wind gusts not reflected in the weather station's average hourly wind speed) or an ecological explanation for the change in flux values over the course of the day. We also note that we do not have alkalinity data for these ponds, but high alkalinity could buffer pH changes that would affect a lack of change in CO_2 concentrations.

Table 6 This study had concentrations, saturation, and efflux values in range of other estimates, though efflux estimates were at the lower end of the range. Studies listed here are those not included in the Holgerson et al. (2017) meta-analysis or those with saturation values reported (e.g., Kortelainen et al. (2006)

Study	Location	Pond type	Pond size (m^2)	CO_2 concentration (umol L^{-1})	CO_2 saturation (%)	CO_2 Efflux (mmol CO_2 m^{-2} h^{-1})
Holgerson et al. (meta-analysis) 2017	Global	All	<1000	133.99 ± 16.69	NA	35.18
Holgerson et al. (meta-analysis) 2017	Global	All	1000–10^4	70.29 ± 14.8	NA	21.21 ± 5.88
Burger et al. 2016	Ontario	Peatland	847	114.8 ± 33.1 (July) 132.0 ± 21.0 (September)	NA	2.95
Kortelainen et al. (2006)	Finland	Permanent lakes	2.6×10^4	114.8	500	0.11
Catalan et al. (2014)	Spain	Temporary ponds	200–2000	NA	NA	5.05 ± 5.75
Obrador et al. (2018)	Spain	Temporary ponds	2000 m^2–173 ha	NA	NA	4.49 ± 4.32
Bortolotti et al. (2016)	Saskatchewan, Canada	Natural semi-permanent wetlands	4130	10.5	NA	19.4 ± 82.4
This study	Subalpine ponds, CO	Various hydroperiods	900–7800	77.6 ± 24.5	625.9 ± 24.5	0.45 ± 0.43

Measured Flux Vs. Wind Speed and Temperature Based Models

Site-specific studies of CO_2 flux generally apply one of the three methods that we compared, whether it be wind-based models (Hamilton et al. 1994; Pelletier et al. 2007), the floating chamber approach (Catalán et al. 2014; Natchimuthu et al. 2014; Gilbert et al. 2017; Obrador et al. 2018), or convection based models (Holgerson et al. 2017). Laurion et al. (2010) also compared wind-based model and chamber-collected estimates of flux and similarly found that wind-based flux estimates were 2.5 to 3 times higher than those measured using floating chambers ($n = 35$). The wind-based models could have led to an overestimate of flux because this model was developed for lakes of longer fetch and where surrounding local topography and vegetation had less of an effect on total flux (Cole and Caraco 1998). The convection-based model averages that we used were more reflective of the physical environment of small ponds (Read et al. 2012). Floating chambers can cause overestimates of CO_2 flux by up to a factor of 2 by creating artificial turbulence in calm conditions in small water bodies (Vachon et al. 2010). However, some floating chamber estimates were more than twice that of the estimates yielded from the convection-based model. Thus, we suspect that the most representative estimates of CO_2 flux from the ponds likely fall between the floating chamber measurements and the modeled flux from the convection-based model.

CO_2 Flux from Pond Water and Previously Wetted Soils during the Ice-Free Season

Carbon dioxide flux from soils of recently dried pond areas was almost an order of magnitude higher than from pond waters, and flux from other soils in the area was twice that of ponds soils, regardless of whether or not those soils had any vegetation. These estimates were in range of other measurements of soil CO_2 flux from surrounding areas (Read et al. 2017),and consistent with the general notion that aerobic fungal and bacterial processing during the dry phase of temporary ponds leads to the rapid removal of annual inputs of organic material and reduces the accumulation of peat (Fuell et al. 2013, Boon et al. 2015). This positive feedback effect of climate change is similar to that which is seen occurring in permafrost regions where permafrost thaw allows microbial decomposition of organic carbon (Schuur et al. 2008). Shifts in pond hydroperiod should also reduce the overall importance of CO_2 flux from animal detritivores, but the relative importance of detritivores and microbial decomposers is poorly understood in shallow lentic habitats and thus it is not clear whether that would result in a net increase or decrease in CO_2 flux.

Because we used floating chambers to estimate CO_2 flux, it is more likely that we overestimated flux rates, in which case the difference between water and soil flux rates is greater. This is contrary to other findings that have compared pond water to pond soil flux in peatlands, where net flux from waters was positive and from soils was negative (Hamilton et al. 1994), but consistent with studies of temporary ponds that found CO_2 flux was higher in recently exposed pond soils (Catalán et al. 2014; Gilbert et al. 2017; Obrador et al. 2018). The difference between flux rates suggested that as some ponds become progressively drier with climate change, and as some permanent ponds continue to transition to being more temporary, we will face a positive feedback loop in CO_2 concentrations (Smol and Douglas 2007).

Recently exposed pond soils were still wet or saturated with pond water because 2017 was an unusually rainy summer and ponds constantly refilled and dried. We suspect that the reason recently exposed soils had lower flux rates than other surrounding soils is that the soils remained saturated (hence anaerobic), slowing rates of respiration. Thus, model findings were conservative and likely underestimates of changes in total flux over a season as pond areas become exposed. As these soils become more routinely aerated as the water table progressively drops, we expect flux to increase to the level of surrounding soils. Indeed, at least one pond at Mexican Cut (e.g., pond 20) has dried enough that it no longer contains common aquatic invertebrates or sedges (S.A. Wissinger unpublished data). Furthermore, our chamber-measured CO_2 flux rates were higher than those calculated from the convection-based models, suggesting that the difference between water and exposed soil flux rates could be even greater than we modeled.

Conclusions

Across an array of adjacent high-elevation temperate shallow ponds and wetlands with different hydroperiods, we found that temporary ponds had higher CO_2 concentrations and higher CO_2 flux over the course of the season than more permanent habitats because these ponds transition to exposed soils as they dry. These ponds are becoming increasingly temporary with longer summer seasons, earlier snowmelt, and higher temperatures, or even with purposeful draining by humans. Considering only instantaneous rates of flux (either measured or modeled) from pond waters misrepresents the estimates necessary for including ponds in the global carbon budget because instantaneous water flux rates do not encompass the total flux from pond areas as they transition to exposed soils. Thus, our findings from this rapidly changing habitat type suggest that climate change could greatly accelerate CO_2 emissions as ponds shift in hydroperiod when we consider entire pond areas over the course of a wetted season.

References

Akaike H (1998) Information Theory and an Extension of the Maximum Likelihood Principle. In: Information theory and an extension of the maximum likelihood principle. Selected papers of Hirotugu Akaike. Springer, pp 199–213

Arnell NW (1999) Climate change and global water resources. Glob Environ Chang 9:S31–S49. https://doi.org/10.1016/S0959-3780(99)00017-5

Baker TT, Lockaby BG, Conner WH, Meier CE, Stanturf JA, Burke MK (2001) Leaf litter decomposition and nutrient dynamics in four southern forested floodplain communities. Soil Sci Soc Am J 65: 1334–1347

Barnett TP, Adam JC, Lettenmaier DP (2005) Potential impacts of a warming climate on water availability in snow-dominated regions. Nature 438:303–309

Barton K, Barton MK (2018) Package 'MuMIn'

Battle JM, Golladay SW (2007) How hydrology, habitat type, and litter quality affect leaf breakdown in wetlands on the gulf coastal plain of Georgia. Wetlands 27:251–260

Batzer DP, Sharitz RR (2014) Ecology of freshwater and estuarine wetlands. Univ of California Press

Batzer DP, Wissinger SA (1996) Ecology of insect communities in nontidal wetlands. Annu Rev Entomol 41:75–100

Billick I Installation, maintenance and publication of data from the RMBL weather stations has been supported by NSF award (MRI-0821369), NSF Grant DBI #0821369, and DOE funding as well as ongoing operational support from RMBL, the upper Gunnison River water Conservancy District and the LBNL science focus area 2.0 project. Rocky Mountain Biological Station

Bonaiuti S, Blodau C, Knorr K-H (2017) Transport, anoxia and end-product accumulation control carbon dioxide and methane production and release in peat soils. Biogeochemistry 133:219–239

Boon PI (2006) Biogeochemistry and bacterial ecology of hydrologically dynamic wetlands. Ecol Freshw Estuar Wetl Univ Calif Press Berkeley 568:

Bortolotti LE, St. Louis VL, Vinebrooke RD, Wolfe AP (2016) Net eco-system production and carbon greenhouse gas fluxes in three Prairie wetlands. Ecosystems 19:411–425. https://doi.org/10.1007/s10021-015-9942-1

Brooks RT (2009) Potential impacts of global climate change on the hydrology and ecology of ephemeral freshwater systems of the forests of the northeastern United States. Clim Chang 95:469–483. https://doi.org/10.1007/s10584-008-9531-9

Burger M, Berger S, Spangenberg I, Blodau C (2016) Summer fluxes of methane and carbon dioxide from a pond and floating mat in a continental Canadian peatland. Biogeosciences 13(12):3777–3791

Burkett V, Kusler J (2000) Climate change: potential impacts and inter-actions in wetlands of the Untted States1. J Am Water Resour Assoc 36:313–320. https://doi.org/10.1111/j.1752-1688.2000.tb04270.x

Carpenter SR, Fisher SG, Grimm NB, Kitchell JF (1992) Global change and freshwater ecosystems. Annu Rev Ecol Syst 23:119–139

Catalán N, von Schiller D, Marcé R et al (2014) Carbon dioxide efflux during the flooding phase of temporary ponds. Limnetica 33:349–360

Clow DW (2010) Changes in the timing of snowmelt and streamflow in Colorado: a response to recent warming. J Clim 23:2293–2306

Clymo RS, Turunen J, Tolonen K (1998) Carbon accumulation in peatland. Oikos 81:368–388

Cole JJ, Caraco NF (1998) Atmospheric exchange of carbon dioxide in a low-wind oligotrophic lake measured by the addition of SF6. Limnol Oceanogr 43:647–656. https://doi.org/10.4319/lo.1998.43.4.0647

Cole JJ, Caraco NF, Kling GW, Kratz TK (1994) Carbon dioxide super-saturation in the surface waters of lakes. Science 265:1568–1570

Cole JJ, Pace ML, Carpenter SR, Kitchell JF (2000) Persistence of net heterotrophy in lakes during nutrient addition and food web manip-ulations. Limnol Oceanogr 45:1718–1730

Cole JJ, Prairie YT, Caraco NF, McDowell WH, Tranvik LJ, Striegl RG, Duarte CM, Kortelainen P, Downing JA, Middelburg JJ, Melack J (2007) Plumbing the global carbon cycle: integrating inland waters into the terrestrial carbon budget. Ecosystems 10:172–185

Corcoran RM, Lovvorn JR, Heglund PJ (2009) Long-term change in limnology and invertebrates in Alaskan boreal wetlands. Hydrobiologia 620:77–89. https://doi.org/10.1007/s10750-008-9616-5

Dodson SI (1982) Chemical and biological limnology of six west-Central Colorado Mountain ponds and their susceptibility to acid rain. Am Midl Nat 107:173–179. https://doi.org/10.2307/2425198

Downing JA, Prairie YT, Cole JJ, Duarte CM, Tranvik LJ, Striegl RG, McDowell WH, Kortelainen P, Caraco NF, Melack JM, Middelburg JJ (2006) The global abundance and size distribution of lakes, ponds, and impoundments. Limnol Oceanogr 51:2388–2397

Duarte CM, Prairie YT (2005) Prevalence of heterotrophy and atmo-spheric CO2 emissions from aquatic ecosystems. Ecosystems 8: 862–870

Elser JJ, Andersen T, Baron JS, Bergstrom AK, Jansson M, Kyle M, Nydick KR, Steger L, Hessen DO (2009) Shifts in lake N: P stoi-chiometry and nutrient limitation driven by atmospheric nitrogen deposition. science 326:835–837

Gilbert PJ, Cooke DA, Deary M, Taylor S, Jeffries MJ (2017) Quantifying rapid spatial and temporal variations of CO 2 fluxes from small, lowland freshwater ponds. Hydrobiologia 793:83–93

Hamilton JD, Kelly CA, Rudd JWM, Hesslein RH, Roulet NT (1994) Flux to the atmosphere of CH4 and CO2 from wetland ponds on the Hudson Bay lowlands (HBLs). J Geophys Res Atmos 99:1495–1510. https://doi.org/10.1029/93JD03020

Helton AM, Bernhardt ES, Fedders A (2014) Biogeochemical regime shifts in coastal landscapes: the contrasting effects of saltwater in-cursion and agricultural pollution on greenhouse gas emissions from a freshwater wetland. Biogeochemistry 120:133–147

Holgerson MA (2015) Drivers of carbon dioxide and methane supersat-uration in small, temporary ponds. Biogeochemistry 124:305–318

Holgerson MA, Raymond PA (2016) Large contribution to inland water CO 2 and CH 4 emissions from very small ponds. Nat Geosci 9: 222–226

Holgerson MA, Farr ER, Raymond PA (2017) Gas transfer velocities in small forested ponds. Journal of Geophysical Research: Biogeosciences 122:1011–1021

Inkley MD, Wissinger SA, Baros BL (2008) Effects of drying regime on microbial colonization and shredder preference in seasonal wood-land wetlands. Freshw Biol 53:435–445

Jackson CR, Thompson JA, Kolka RK (2014) Wetland soils, hydrology and geomorphology. In: Batzer, D.; Sharitz, R., eds. Ecology of freshwater and estuarine wetlands. Berkeley, CA: University of California Press: 23-60. Chapter 2:23–60

Kelly CA, Fee E, Ramlal PS, Rudd JWM, Hesslein RH, Anema C, Schindler EU (2001) Natural variability of carbon dioxide and net epilimnetic production in the surface waters of boreal lakes of dif-ferent sizes. Limnol Oceanogr 46:1054–1064

Kortelainen P, Rantakari M, Huttunen JT et al (2006) Sediment respiration and lake trophic state are important predictors of large CO2 evasion from small boreal lakes. Glob Chang Biol 12:1554–1567. https://doi.org/10.1111/j.1365-2486.2006.01167.x

Kragh T, Andersen MR, Sand-Jensen K (2017) Profound afternoon depression of ecosystem production and nighttime decline of respiration in a macrophyte-rich, shallow lake. Oecologia 185:157–170. https://doi.org/10.1007/s00442-017-3931-3

Laurion I, Vincent WF, MacIntyre S, Retamal L, Dupont C, Francus P, Pienitz R (2010) Variability in greenhouse gas emissions from permafrost thaw ponds. Limnol Oceanogr 55:115–133. https://doi.org/10.4319/lo.2010.55.1.0115

Lee S-Y, Ryan ME, Hamlet AF, Palen WJ, Lawler JJ, Halabisky M (2015) Projecting the hydrologic impacts of climate change on montane wetlands. PLoS One 10:e0136385

Lund JO, Wissinger SA, Peckarsky BL (2016) Caddisfly behavioral responses to drying cues in temporary ponds: implications for effects of climate change. Freshwater Science 35:619–630

Magnusson AK, Williams DD (2006) The roles of natural temporal and spatial variation versus biotic influences in shaping the physicochemical environment of intermittent ponds: a case study. Arch Hydrobiol 165:537–556

Natchimuthu S, Selvam BP, Bastviken D (2014) Influence of weather variables on methane and carbon dioxide flux from a shallow pond. Biogeochemistry 119:403–413

Obrador B, von Schiller D, Marcé R, Gómez-Gener L, Koschorreck M, Borrego C, Catalán N (2018) Dry habitats sustain high CO 2 emissions from temporary ponds across seasons. Sci Rep 8:3015

Pelletier L, Moore TR, Roulet NT, Garneau M, Beaulieu-Audy V (2007) Methane fluxes from three peatlands in the La Grande Riviere watershed, James Bay lowland, Canada. J Geophys Res Biogeosci 112

Pinheiro J, Bates D, DebRoy S, Sarkar D (2014) R Core team (2014) nlme: linear and nonlinear mixed effects models. R package version 3.1–117. Available H TtpCRAN R-Proj. Orgpackage Nlme

Post WM, Emanuel WR, Zinke PJ, Stangenberger AG (1982) Soil carbon pools and world life zones. Nature 298:156–159. https://doi.org/10.1038/298156a0

Power ME, Stout RJ, Cushing CE, Harper PP, Hauer FR, Matthews WJ, Moyle PB, Statzner B (1988) Biotic and abiotic controls in river and stream communities. J N Am Benthol Soc 7:456–479

R Core Team (2016) R: a language and environment for statistical computing. R Foundation for Statistical Computing, Vienna, Austria

Read JS, Hamilton DP, Desai AR, Rose KC, MacIntyre S, Lenters JD, Smyth RL, Hanson PC, Cole JJ, Staehr PA, Rusak JA, Pierson DC, Brookes JD, Laas A, Wu CH (2012) Lake-size dependency of wind shear and convection as controls on gas exchange. Geophys Res Lett 39

Read QD, Henning JA, Classen AT, Sanders NJ (2017) Aboveground resilience to species loss but belowground resistance to nitrogen addition in a montane plant community. J Plant Ecol:rtx015

Resh VH, Brown AV, Covich AP, Gurtz ME, Li HW, Minshall GW, Reice SR, Sheldon AL, Wallace JB, Wissmar RC (1988) The role of disturbance in stream ecology. J N Am Benthol Soc 7:433–455

Schuur EA, Bockheim J, Canadell JG et al (2008) Vulnerability of permafrost carbon to climate change: implications for the global carbon cycle. AIBS Bull 58:701–714

Serreze MC, Clark MP, Armstrong RL, McGinnis DA, Pulwarty RS (1999) Characteristics of the western United States snowpack from snowpack telemetry (SNO) data. Water Resour Res 35:2145–2160

Smol JP, Douglas MS (2007) Crossing the final ecological threshold in high Arctic ponds. Proc Natl Acad Sci 104:12395–12397

Strachan SR, Chester ET, Robson BJ (2014) Microrefuges from drying for invertebrates in a seasonal wetland. Freshw Biol 59:2528–2538

Thompson SK (2012) Sampling. John Wiley & Sons

Tuytens K, Vanschoenwinkel B, Waterkeyn A, Brendonck L (2014) Predictions of climate change infer increased environmental harshness and altered connectivity in a cluster of temporary pools. Freshw Biol 59:955–968. https://doi.org/10.1111/fwb.12319

Vachon D, Prairie YT, Cole JJ (2010) The relationship between near-surface turbulence and gas transfer velocity in freshwater systems and its implications for floating chamber measurements of gas exchange. Limnol Oceanogr 55:1723–1732

Verpoorter C, Kutser T, Seekell DA, Tranvik LJ (2014) A global inventory of lakes based on high-resolution satellite imagery. Geophys Res Lett 41:6396–6402

Wanninkhof R (1992) Relationship between wind speed and gas exchange over the ocean. J Geophys Res Oceans 97:7373–7382

Weiss R (1974) Carbon dioxide in water and seawater: the solubility of a non-ideal gas. Mar Chem 2:203–215

Wellborn GA, Skelly DK, Werner EE (1996) Mechanisms creating community structure across a freshwater habitat gradient. Annu Rev Ecol Syst 27:337–363

Williamson CE, Saros JE, Vincent WF, Smol JP (2009) Lakes and reservoirs as sentinels, integrators, and regulators of climate change. Limnol Oceanogr 54:2273–2282. https://doi.org/10.4319/lo.2009.54.6_part_2.2273

Wissinger SA, Oertli B, Rosset V (2016) Invertebrate Communities of Alpine Ponds. In: Invertebrate communities of alpine ponds. Invertebrates in freshwater wetlands. Springer, Cham, pp 55–103

Wissinger SA, Whiteman HH, Sparks GB et al (1999) Foraging trade-offs along a predator–permanence gradient in subalpine wetlands. Ecology 80:2102–2116